

The final phase of inspiral of strange quark star binaries

Dorota Gondek-Rosińska^{1,*} and François Limousin^{2,†}

¹*Institute of Astronomy, University of Zielona Góra, Lubuska 2, 65-265, Zielona Góra, Poland,
Laboratoire de l'Univers et de ses Théories, UMR 8102 du C.N.R.S., Observatoire de Paris, F-92195 Meudon Cedex, France,
Departament de Física Aplicada, Universitat d'Alacant, Apartat de correus 99, 03080 Alacant, Spain*

²*Center for Radiophysics and Space Research, Cornell University, Ithaca, New York, 14853, USA,
Laboratoire de l'Univers et de ses Théories, UMR 8102 du C.N.R.S., Observatoire de Paris, F-92195 Meudon Cedex, France*

(Dated: 30 January 2008)

We present calculations of the final phase of inspiral of irrotational strange star binaries. Two types of equation of state at zero temperature are used - the MIT bag model and the Dey et al. 1998 model of strange quark matter. We study the precoalescence stage within the Isenberg-Wilson-Mathews approximation of General Relativity using a multidomain spectral method. The gravitational-radiation driven evolution of the binary system is approximated by a sequence of quasi-equilibrium configurations at a fixed baryon number and with decreasing separation. We find that the innermost stable circular orbit (ISCO) is determined always by an orbital instability for binaries consisting of two stars built predominantly of strange quark matter independently on the total mass of a binary system and compactness parameter of each star. In contrast, for neutron stars described by baryonic equation of state without exotic phases the ISCO is given by the mass-shedding limit. The gravitational wave frequency at the ISCO, which marks the end of the inspiral phase, is always higher than 1.1kHz for equal masses irrotational strange quark stars with the total mass-energy of a binary system greater than $2M_{\odot}$. We find that the dependence of the frequency of gravitational waves at the ISCO on the compactness parameter for the equal mass binaries can be described by the same simple analytical formulae for broad ranges of masses independently on a strange star model. Detailed comparisons with binary neutrons star models, as well as with the third order Post-Newtonian point-mass binaries are given. The difference in the phase, for two $1.35M_{\odot}$ strange stars, between our numerical results and 3PN is $\sim 40\%$ for the last two orbits of inspiral.

PACS numbers: 04.40.Dg, 04.30.Db, 04.25.Dm, 97.10.Kc, 97.60.Jd

I. INTRODUCTION

Coalescing compact object binaries are the strongest and hence the most promising sources of gravitational waves (GW) for LIGO, VIRGO and other interferometric detectors [1, 2, 3]. Among these, binary neutron stars have been a subject of extreme interest since the GW signal of terminal phases of evolution of such binary system could yield important information about the equation of state (EOS) at nuclear densities (e.g [4, 5, 6, 7, 8, 9, 10, 11]). One can impose constraints on the EOS of neutron stars using a simple method based on the properties of quasiequilibrium binary sequences [5, 8, 9]. The individual masses of the two neutron stars in a binary system can be determined taking into account the frequency evolution of the GW signal of the inspiral phase and high-order PN effects on the phase evolution of the signal [12]. In addition the compactness parameter M/R , hence R , of neutron stars (where M is gravitational mass and R stellar radius of an isolated neutron star) can be found based on the observed deviation of the gravitational energy spectrum of a quasiequilibrium sequence from point-mass behavior at the end of inspiral [5].

Several groups have studied the last orbits of inspiraling binary neutron stars in the quasi-equilibrium approximation, and in the framework of Isenberg-Wilson-Mathews (IWM) approximation of general relativity (see [13] for a review). The quasi-equilibrium assumption approximates the evolution of the system by a sequence of exactly circular orbits (as the time evolution of the orbit is much larger than the orbital period). The IWM approximation amounts to using a conformally flat spatial metric, which reduces the problem to solving only five of the ten Einstein equations. The equilibrium configurations have been calculated for irrotational binaries since the viscosity of neutron star matter is far too low to ensure synchronization during the late stage of the inspiral [14, 15].

In order to construct accurate templates of expected GW signal from neutron stars binaries one has to take into account realistic description of nuclear matter and astrophysically relevant masses of neutron stars in a binary system.

Almost all relativistic studies of the final phase of the inspiral of close binary neutron stars systems employ a simplified EOS of dense matter, namely a polytropic EOS [5, 6, 16, 17, 18, 19, 20, 21, 22, 23]. There are only three exceptions: (i) Oechslin et al. have used a pure nuclear matter EOS, based on a relativistic mean field model and a 'hybrid' EOS with a phase transition to quark matter at high density [10]; (ii) Bejger et al. have computed quasi-equilibrium sequences based on three nuclear matter EOS

*Electronic address: Dorota.Gondek@obspm.fr

†Electronic address: limousin@astro.cornell.edu

[9] iii) Limousin et al. have studied the properties of binary strange quark stars described by the simplified MIT bag model (with massless and not interacting quarks) of strange quark matter [8]. In these three papers the authors have considered only binary systems consisting of two identical stars. The assumption of almost equal masses of neutron stars in a binary system was based on the current set of well-measured neutron stars masses in relativistic binary radio pulsars. However, one has to note that the conclusions based on analysis of properties of radio binary pulsars suffer from small number statistics and from several selection effects [24, 25].

In this article we calculate the final phase of inspiral of irrotational strange quark star binaries using the MIT bag model and the Dey et al. (1998)[26] model of strange quark matter. We study the impact of the equation of state and total energy-mass on the last orbits of binary strange quark stars. We compare the evolution of strange star binaries with neutron star binaries in order to find any characteristic features in the gravitational signal that will help to distinguish between strange stars and neutron stars.

The paper is organized in the following way: Sec. II is devoted to the description of the EOSs used to describe strange stars. Sec. III is a brief summary of the assumptions upon which this work is based and a short description of the basic equations for quasi-equilibrium configurations. In Sec. IV we comment on the properties of evolutionary sequences and define the notion of innermost stable circular orbit. In Sec. V we present the numerical results for irrotational strange stars binaries of $M = 1.35M_\odot$ and compare their evolution with that of neutron stars. Then in Sec. VI we show the results obtained for binary strange stars with different total mass and compare them with neutron star binaries. Section VII contains the final discussion.

Throughout the paper, we use geometrized units, for which $G = c = 1$, where G and c denote the gravitational constant and speed of light respectively.

II. EQUATIONS OF STATE AND STELLAR MODELS

Strange quark stars (SQS) are currently considered as a possible alternative to neutron stars as compact objects (see e.g. [27, 28, 29] and references therein). Typically, strange stars are modeled with an EOS based on the MIT-bag model (e.g. [30, 31]) in which quark confinement is described by an energy term proportional to the volume [32]. There are three physical quantities entering the MIT-bag model: the mass of the strange quarks, m_s , the bag constant, B , and the strength of the QCD coupling constant α . In the framework of this model the quark matter is composed of massless u and d quarks, massive s quarks and electrons. We performed calculations for three different sets of parameters of the MIT-bag model:

EOS	$M[M_\odot]$	$M_B[M_\odot]$	R [km]	M/R
SQSB40 $a = 0.324, \rho_0 = 3.0563,$ $n_0 = 0.19611$	0.5	0.5611	9.001	0.0820
	1.35	1.6081	12.09	0.1648
	1.5	1.805	12.41	0.1784
	1.75	2.1434	12.84	0.2011
SQSB60 $a = 1/3, \rho_0 = 4.2785,$ $n_0 = 0.28665$	0.5	0.5899	8.026	0.0920
	1	1.2296	9.877	0.1495
	1.35	1.7076	10.68	0.1867
	1.65	2.1406	11.10	0.2196
SQSB56 $a = 0.301, \rho_0 = 4.4997,$ $n_0 = 0.27472$	0.5	0.5383	7.865	0.0939
	0.7	0.7668	8.709	0.1187
	1	1.1233	9.637	0.1532
	1.2	1.3707	10.09	0.1756
	1.35	1.5620	10.35	0.1925
	1.5	1.7587	10.54	0.2101
DSQS $a = 0.463, \rho_0 = 11.53,$ $n_0 = 0.725$	1.35	1.7191	7.336	0.2717

TABLE I: Global parameters of isolated static strange stars for the four models of strange stars used in our computations. The symbols have following meaning: M is the gravitational mass, M_B the baryon mass, R stellar radius, $M/R \equiv GM/Rc^2$ is the compaction parameter. The mass density ρ_0 and baryon density n_0 at zero pressure are in units [10^{14} g/cm 3] and [fm^{-3}] respectively.

- i) **SQSB56** - the standard MIT bag model: $m_s c^2 = 200$ MeV, $\alpha = 0.2$, $B = 56$ MeV/fm 3 ;
- ii) **SQSB60** - the simplified MIT bag model with $m_s = 0$, $\alpha = 0$; $B = 60$ MeV/fm 3 ;
- iii) **SQSB40** - the "extreme" MIT bag model (relatively low strange quark mass and B but high α): $m_s c^2 = 100$ MeV, $\alpha = 0.6$, $B = 40$ MeV/fm 3 .

The second type of EOS which we employ is the Dey et al. (1998) EOS of strange quark matter. In this model, quarks of the density dependent mass are confined at zero pressure and deconfined at high density. The quark interaction is described by an interquark vector potential originating from gluon exchange, and by a density dependent scalar potential which restores the chiral symmetry at high densities. This model, with an appropriate choice of the EOS parameters, gives absolutely stable strange quark matter. Two cases of this model have been used in the literature SS1 and SS2 - both giving a rather low value for the maximum gravitational mass $M_{\text{max}} = 1.33 M_\odot$ and $M_{\text{max}} = 1.44 M_\odot$ respectively. We have chosen the SS2 model and call it **DSQS** in our paper. The stars described by the Dey et al. (1998) model

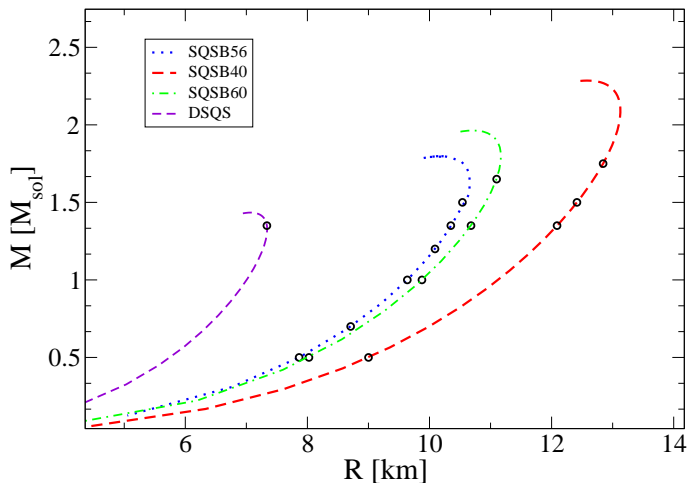


FIG. 1: Gravitational mass M versus stellar radius R for sequences of static isolated strange quark stars described by three different sets of parameters of the MIT-bag model and by the Dey et al. (1998) model. The circles correspond to stellar configurations considered in calculations of equal-mass evolutionary sequences.

are very compact i.e. the gravitational redshifts z for the maximum mass configurations are much larger than those for strange stars within the MIT bag model (also larger than z for most models of neutron stars).

It was shown that different strange quark EOS can be fitted very well by following formulas [33, 34]:

$$p = a(\rho - \rho_0), \quad (1)$$

$$n(p) = n_0 \cdot \left[1 + \frac{1+a}{a} \frac{p}{\rho_0} \right]^{1/(1+a)}, \quad (2)$$

where p , ρ , n are the pressure, the mass density and the baryon density respectively and a , ρ_0 , n_0 are some constants. In general this equation corresponds to a self-bound matter with mass density ρ_0 and baryon density n_0 at zero pressure and with a fixed sound velocity \sqrt{a} at all pressures. The parameters a and ρ_0 and n_0 for each EOS used in the paper are given in Table I. The strange stars described by the DSQS model have very high density at the surface $\rho_0 = 1.15 \times 10^{15}$ [g/cm³]. For the MIT bag model ρ_0 is in the range $\sim 3 - 6.4$ [10^{14} g/cm³] [29, 34]. The parameter a is found to be between 0.289 and 1/3 (for $0 \leq \alpha \leq 0.6$ and $0 \leq m_s \leq 250$ MeV) [34] for the MIT bag model and 0.463 for DSQS model [33]. The higher value of a and ρ_0 the higher compactness parameter of a star with fixed gravitational mass.

In Fig. 1 we present gravitational mass versus stellar radius for sequences of static strange quark stars. Circles correspond to configurations studied in the paper. The global parameters are given in Table I. Depending on the model we obtain the radius of a $1.35 M_\odot$ star in the range 7-13 km.

III. ASSUMPTIONS AND METHODS

A. Assumptions

The first assumption regards the matter stress-energy tensor \mathbf{T} , which we assume to have the *perfect fluid* form:

$$\mathbf{T} = (e + p)\mathbf{u} \otimes \mathbf{u} + p\mathbf{g}, \quad (3)$$

where e , p , \mathbf{u} and \mathbf{g} are respectively the fluid proper energy density, the fluid pressure, the fluid 4-velocity, and the spacetime metric. This constitutes an excellent approximation for neutron star matter or strange star matter.

The last orbits of inspiraling binary compact stars can be studied in the *quasi-equilibrium* approximation. Under this assumption the evolution of a system is approximated by a sequence of exactly circular orbits. This assumption results from the fact that the time evolution of an orbit is still much larger than the orbital period and that the gravitational radiation circularizes an orbit of a binary system. This implies a continuous spacetime symmetry, called *helical symmetry* [35, 36] represented by the Killing vector

$$\ell = \frac{\partial}{\partial t} + \Omega \frac{\partial}{\partial \varphi}, \quad (4)$$

where Ω is the orbital angular velocity and $\partial/\partial t$ and $\partial/\partial \varphi$ are the natural frame vectors associated with the time coordinate t and the azimuthal coordinate φ of an asymptotic inertial observer.

We also assume that the spatial part of the metric (i.e. the metric induced by \mathbf{g} on each hypersurface Σ_t) is conformally flat, which corresponds to the *Isenberg-Wilson-Mathews* approximation to general relativity [37, 38, 39] (see Ref. [36] for a discussion). Thanks to this approximation we have to solve only five of the ten Einstein equations.

The fourth assumption concerns the fluid motion inside each star. We only consider *irrotational* motion (assuming that the fluid has zero vorticity in the inertial frame).

B. Equations to be solved

We just mention briefly all the equations we have to solve and refer the reader to Limousin et al. [8] for more details.

The gravitational field equations have been obtained within the 3+1 decomposition of the Einstein's equations [40, 41], using the extended conformal thin sandwich formalism [42] and taking into account the helical symmetry of the spacetime. This gives one vectorial elliptic equation for the shift vector N^i coming from the momentum constraint and two scalar elliptic equations for $\nu = \ln N$ and $\beta = \ln(AN)$, coming from the trace of the spatial part of the Einstein equations combined with the Hamiltonian constraint, N being the lapse function

and A the conformal factor.

Apart from the gravitational field equations, we have to solve the fluid equations. The equations governing the quasi-equilibrium state are the relativistic Euler equation and the equation of baryon number conservation. Irrotational motion admit a first integral of the relativistic Euler equation:

$$H + \nu - \ln \Gamma_0 + \ln \Gamma = \text{const.}, \quad (5)$$

where H is the pseudoenthalpy, Γ_0 is the Lorentz factor between the co-orbiting and the Eulerian observers and Γ is the Lorentz factor between the fluid and the co-orbiting observers.

The equation of baryon number conservation is written as an elliptic equation for the velocity potential Ψ . The method of solving this equation is different for neutron stars and strange stars. For strange stars, we have to impose a Neumann-like boundary condition for the velocity potential at the surface of the star (see paragraph IV.C of [8] for details) to have flow field tangent to the surface in a rotating frame.

C. Numerical method

The resolution of the above nonlinear elliptic equations is performed thanks to a numerical code based on multidomain spectral methods and constructed upon the *LORENE* C++ library [43]. The detailed description of the whole algorithm, as well as numerous tests of the code can be found in [23]. Additional tests have been presented in Sec. 3 of [6]. The code has already been used successfully for calculating the final phase of inspiral of binary neutron stars described by polytropic EOS [5, 6, 16, 21, 44, 45], realistic EOS [7, 9] as well as binary strange stars [7, 8]. It is worth to stress that the adaptation of the domains (numerical grids) to the stellar surface (surface-fitted coordinates) used in the code is very important for calculating binary systems of strange stars. This method enable us to treat the strongly discontinuous density profile at the surface of a strange star and avoid any Gibbs-like phenomenon. [46].

We used one numerical domain for each star and 3 (resp. 4) domains for the space around them for a small (resp. large) separation between stars. In each domain, the number of collocation points is chosen to be $N_r \times N_\theta \times N_\varphi = 25 \times 17 \times 16$, where N_r , N_θ , and N_φ denote the number of collocation points (= number of polynomials used in the spectral method) in the radial, polar, and azimuthal directions respectively.

The convergence of the procedure is monitored by computing the relative difference $\delta H/H$ between the enthalpy fields at two successive steps. The iterative procedure is stopped when $\delta H/H$ goes below a certain threshold, typically 10^{-7} . The accuracy of the computed models is estimated using a relativistic generalization of the virial

theorem [36]. The virial relative error was found to be a few times 10^{-5} for the closest configurations.

IV. EVOLUTIONARY SEQUENCES

The evolution of a binary system of compact objects is entirely driven by gravitational radiation and can be roughly divided into three phases : point-like inspiral, *hydrostationary inspiral* and merger. The first phase corresponds to large orbital separation (much larger than the neutron star radius) and can be treated analytically using the post-Newtonian (PN) approximation to general relativity (see Ref. [47, 48] for a review). In the second phase the orbital separation becomes only a few times larger than the radius of the star, so the effects of tidal deformation, finite size and hydrodynamics play an important role. In this phase, since the shrinking time of the orbital radius due to the emission of gravitational waves is still larger than the orbital period, it is possible to approximate the state as quasi-equilibrium [16, 49]. The final phase of the evolution is the merger of the two objects, which occur at the dynamical timescale [50, 51, 52, 53]. The quasi-equilibrium computations from the second phase provide valuable initial data for the merger [10, 17, 50, 52].

We focus on the last orbits of the inspiral phase (the hydrostationary inspiral). In this section, we present the numerical results for evolutionary sequences of close strange stars binaries described by three different sets of parameters of the MIT bag model and the Dey model introduced in Sect. II. We consider only equal-mass binary systems with different total masses. By evolutionary sequence, we mean a sequence of quasi-equilibrium configurations of decreasing separation and with constant baryon mass M_B , which are expected to approximate the true evolution of a binary system. In order to investigate the properties of the GW emission during the final phase of binary strange star inspiral we focus on the variation of the ADM (Arnowitt-Deser-Misner, see e.g.[6]) mass of the system M_{ADM} (the total binary mass-energy) with respect to the GW frequency. These two quantities are sufficient to determine the GW energy spectrum. The orbital binding energy is defined by

$$E_{\text{bind}} := M_{\text{ADM}} - M_\infty, \quad (6)$$

where M_∞ is the ADM mass of the system at infinite separation, that is the sum of the gravitational masses, M , of isolated static stars. The variation of E_{bind} along an evolutionary sequence corresponds to the loss of energy via gravitational radiation. Gravitational waves are emitted at twice the orbital frequency: $f_{\text{GW}} = 2f = \Omega/\pi$.

The physical inspiral of binary compact stars terminates by either the orbital instability (turning point of E_{bind}) or the mass-shedding limit (when a cusp forms at the stellar surface in the direction of the companion

(Roche lobe overflow)). In both cases, this defines the *innermost stable circular orbit*. The frequency of gravitational waves at the ISCO is one of potentially observable parameters by the gravitational wave detectors. In addition so called “*break frequencies*”, characteristic frequencies where the power emitted in gravitational waves decreases measurably could be observable quantities [5, 54] and section V. C at this paper.

V. RESULTS FOR EQUAL-MASS STRANGE STAR BINARIES WITH $M_\infty = 2.7 M_\odot$

In Fig. 2 we present the orbital binding energy as a function of gravitational wave frequency along evolutionary sequences of strange quark stars with the total mass-energy in infinite separation $M_\infty = 2 \times 1.35 M_\odot = 2.7 M_\odot$. The different symbols (triangles, stars, diamonds and squares) indicate the individual equilibrium configurations calculated numerically. The big diamonds correspond to the minimum of the binding energy of an evolutionary sequence. A turning point of E_{bind} along an evolutionary sequence indicate an orbital instability [36]. This instability can originate both from relativistic effects (the well-known $r = 6M$ last stable orbit of Schwarzschild metric) and hydrodynamical effects [20].

We present also the 3rd order point masses post-Newtonian (PN) approximation derived by Blanchet [57] (solid line). Comparison of our numerical results with the 3PN calculations reveals a good agreement for small frequencies (large separations). The deviation from PN curves at higher frequencies (smaller separation) is due to hydrodynamical effects, which are not taken into account in the PN approach. The relative difference between binding energy of quasiequilibrium sequences of two $1.35 M_\odot$ strange stars and the 3PN point-mass calculation, caused by the finite size effects, at the frequency of gravitational waves corresponding to the quasiequilibrium ISCO is $\sim 7\%$.

A turning point of E_{bind} is found for each of the three binary strange stars described by the MIT bag model but by the DSQS. For the DSQS model we had to finish our calculations before the orbital instability was reached since for closer configurations we were not able to obtain required accuracy due to very high compactness parameter for this strange quark model. The shape of the MIT bag model strange stars at the ISCO and the closest computed configuration in the case of DSQS model are presented in Fig. 3. The stars for DSQS model are in fact still nearly spherical. One can thus suppose that the turning point should exist for the DSQS model of strange matter in high frequencies. The frequency of gravitational waves at the ISCO for the MIT bag model is found to be in the range $\sim 1130 - 1470\text{Hz}$. The 3PN results for point masses derived by different authors give ISCO at very high frequencies of gravitational waves $> 2 \text{ kHz}$ [55, 56, 57]

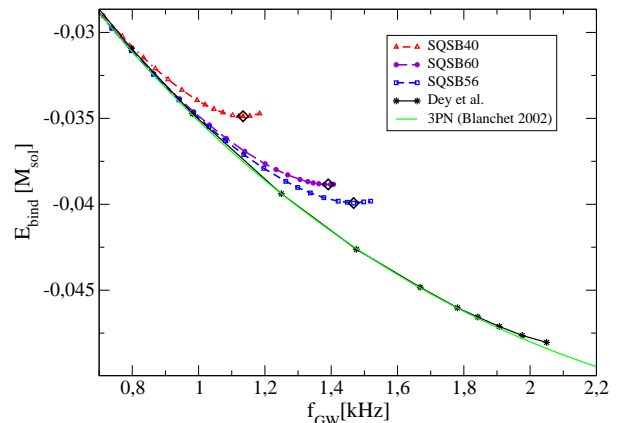


FIG. 2: Orbital binding energy $E_{\text{bind}} = M_{\text{ADM}} - 2M$ as a function of gravitational wave frequency (twice the orbital frequency) along evolutionary sequences of irrotational equal mass (of $1.35 M_\odot$) strange star binaries described by the four EOS introduced in Section II. The solid line corresponds to the 3rd post-Newtonian point masses approximation derived by Blanchet [57].

A. The impact of EOS on the GW frequency at ISCO

It was already suggested by many authors that the frequency of GW at the ISCO depends on the compactness parameter and thus on EOS of nuclear matter. In Fig. 4. we present the frequency of GW at ISCO as a function of compactness parameter for equal-mass binary (consisting of two $1.35 M_\odot$) strange stars described by the MIT bag model and neutron stars described by three nuclear EOS (GNH3 EOS [58], APR EOS [59], BPAL12 EOS [60, 61]- see [9] for details) and by polytropic EOS with $\gamma = 2$ [5].

All evolutionary sequences of binary strange stars terminate at the dynamical orbital instability while equilibrium sequences of binary neutron stars at the mass-shedding limit (for polytropic EOS with $\gamma \leq 2.5$ the ISCO is given by the mass-shedding limit otherwise by the orbital instability [6, 20]). For all EOS the higher compactness of a star is, the higher frequency of gravitational waves at the ISCO is.

We see that for equal-mass evolutionary sequences with the same total mass the dependence $f_{\text{GW,ISCO}}$ versus the compactness parameter can be described by linear function $y = A1x + A2$ for all EOS, where A1 is found to be 11.97, 9.09, 9.165 and A2: -0.841, -0.469, -0.466 for SS binaries, NS described by realistic EOS and polytropic NS binaries respectively. We see that the results obtained for polytropic EOS fit quite well the calculations performed for neutron stars described by realistic EOS. Indeed as found by Bejger et al. 2005 [9] the frequency of grav-

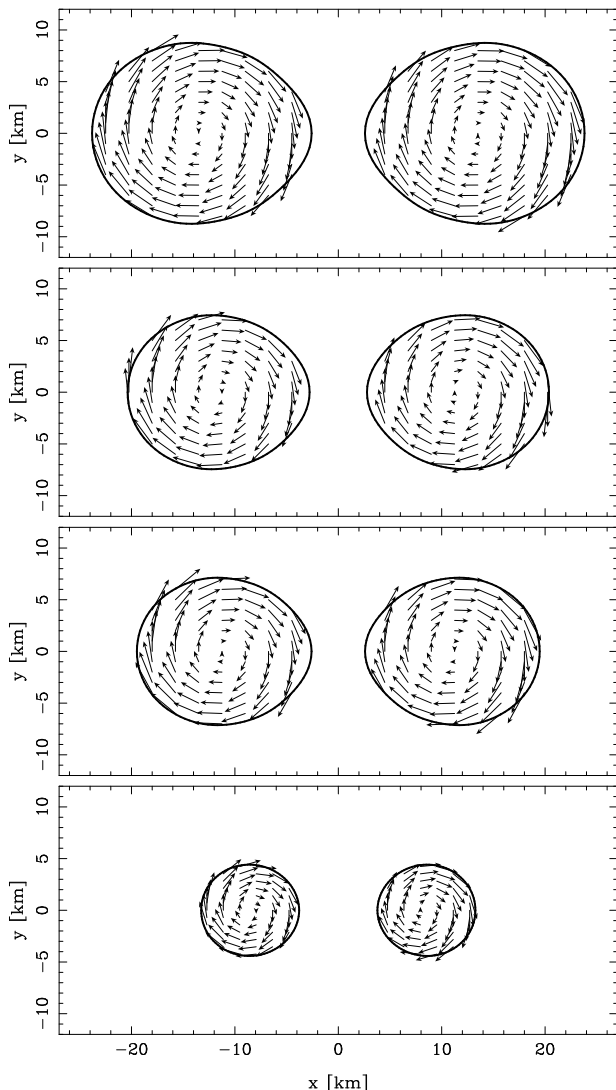


FIG. 3: Velocity field with respect to the co-orbiting frame in the orbital plane for strange stars at the coordinate separation corresponding to ISCO (three upper panels) or to the closest calculated configuration (the lowest panel). The panels correspond to three types of the MIT bag model, SQSB40, SQSB60, SQSB56 and Dey et al. (1998) EOS SQSD from the upper to the lower one respectively. The thick solid lines denote stellar surfaces.

itational waves at the end point of inspiraling neutron stars described by several realistic EOS without exotic phases (such as meson condensates or quark matter) can be predicted, in a good approximation, by studying binaries with assumed polytropic EOSs with $\gamma = 2$ or 2.5. As found by Limousin et al. [8] it wasn't the case for inspiraling strange star binaries which are self-bound objects having very large adiabatic index in the outer layers. The frequency of gravitational waves at the end of inspiral phase is higher by ~ 150 Hz for irrotational strange star binaries than for the polytropic neutron star binaries with the same gravitational mass and stellar radius

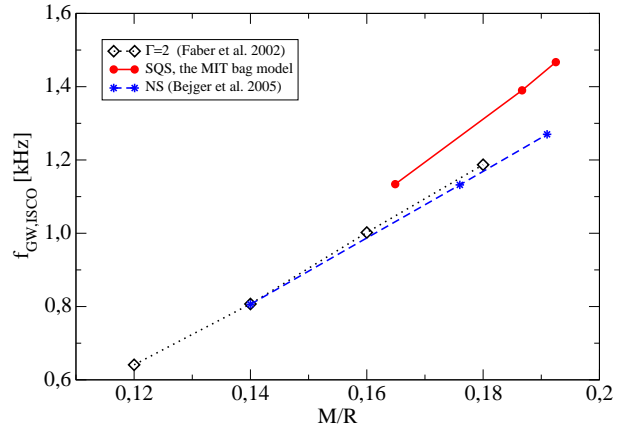


FIG. 4: The frequency of ISCO (the dynamical orbital instability for strange quark stars or the mass-shedding limit for neutron stars) versus compactness parameter for equal-mass (of $1.35M_{\odot}$) strange stars and neutron stars described by realistic EOS [9] and polytropic EOS [5]

in infinite separation. The differences in the evolution of binary strange stars and neutron stars stem from the fact that strange stars are principally bound by another force than gravitation: the strong interaction between quarks. Thanks to this, at the end of the inspiral phase, neutron stars are, for the same separation, more oblate than strange stars. And thus a cusp forms at the stellar surface of neutron stars, which marks the beginning of exchange of matter between the two stars, whereas the surface of strange stars is smooth even at the dynamical instability (see Fig. 3).

The frequency at the end point of inspiral of binary neutron stars described by three nuclear EOS ranges from 806 Hz for GNH3 EOS ($M/R = 0.14$) to 1270 Hz for BPAL 12 EOS ($M/R = 0.191$). The range of frequencies at the ISCO for binary neutron stars intersects with these for binary strange stars (higher than 1130 Hz). The determination of the gravitational wave frequency at the ISCO by the laser interferometers allows to impose constraints on the EOS of matter at ultra-high densities but it is not sufficient to distinguish completely between strange stars and neutron stars. The detection of high value of $f_{\text{GW,ISCO}}$ e.g. 1250 Hz from binary system consisting of two $1.35 M_{\odot}$ stars could indicate the compactness parameter 0.175 or 0.189 depending on EOS.

B. Analytical fits to numerical results

As already mentioned the 3PN calculations reproduce quite well our results for small frequencies (large separations). For close separation we see the deviation from point-mass calculations due to hydrodynamical effects. The observed deviation of the GW energy spectrum for quasiequilibrium sequences (given by the derivative $dE_{\text{bind}}/df_{\text{GW}}$) from point-mass behavior gives also important information about EOS of neutron stars in addition to the frequency of GW at the ISCO [5].

Following Faber et. al. (2002) [5] and Bejger et. al. (2005) [9], we perform some polynomial fits (see below) to each of the computed evolutionary sequences in order to obtain functions required for the GW energy spectrum. The two different approaches were used by authors to represent the variation of the total mass energy as a function of GW frequency. Faber et. al. (2002) [5] fitted the numerical results taking into account 3 terms: $f^{2/3}$, f and f^2 representing the Newtonian point-mass behavior, the lowest order post-Newtonian and finite-size corrections, the tidal interaction energy respectively. However Bejger et. al. (2005) [9] found that it is possible to find much better approximations of numerical results taking into account higher order PN terms. They have shown that the difference between the binding energy of equal-mass of $1.35 M_{\odot}$ irrotational neutron star binaries and the binding energy of binary point masses in the 3PN approximation of Blanchet (2002) [57] can be fitted very well by the power-law dependence on frequency f_{GW} :

$$E_{\text{bind}} - E_{\text{bind}}^{3\text{PN}} = A \left(\frac{f_{\text{GW}}}{1000\text{Hz}} \right)^n. \quad (7)$$

The 3PN formula as obtained by Blanchet [57] from the standard post-Newtonian expansion reads

$$\frac{E_{\text{bind}}^{3\text{PN}}}{M_{\infty}} = -\frac{1}{8}\Omega_*^{2/3} + \frac{37}{384}\Omega_*^{4/3} + \frac{1069}{3072}\Omega_*^2 + \frac{5}{3072} \left(41\pi^2 - \frac{285473}{864} \right) \Omega_*^{8/3}, \quad (8)$$

where Ω_* is the orbital angular frequency expressed in geometrized units:

$$\Omega_* := 2\pi M_{\infty} f = 2\pi M f_{\text{GW}} = 2M\Omega. \quad (9)$$

The terms in $\Omega_*^{2/3}$, $\Omega_*^{4/3}$, Ω_*^2 and $\Omega_*^{8/3}$ in Eq. (8) are respectively the Newtonian, 1PN, 2PN and 3PN term.

In Fig. 5, we present the difference between our numerical results and the 3PN approximation given by Eq. (8). Looking at the scale of Fig. 5, we see that the formula (8) approximates very well the behavior of a binary system of strange stars for a large range of frequencies.

Because of the steep character of the function $E_{\text{bind}} - E_{\text{bind}}^{3\text{PN}}$ seen in Fig. 5, the power n is quite large. The values are listed in Table II. We didn't assume the integer number of the power n . We note that the values of the

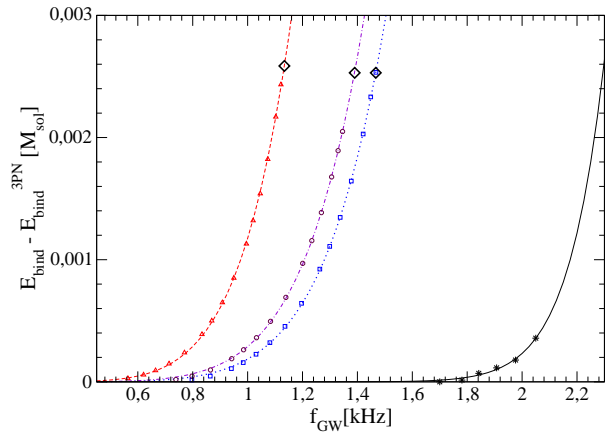


FIG. 5: Difference $E_{\text{bind}} - E_{\text{bind}}^{3\text{PN}}$ between the binding energy of equal-mass of $1.35 M_{\odot}$ irrotational strange quark star binaries and the binding energy of binary point masses in the 3PN approximation of Blanchet (2002) [57]. The different symbols (triangles, circles, squares and stars) correspond to the numerical results, lines to polynomial fits (7) to them and big diamonds to ISCO.

power n are similar for the three EOS of MIT bag model. So we also done fits for an intermediate value $n = 6.5$ for these three EOS and denote by $A_{n=6.5}$ its corresponding factor. The information on the frequency of departure from 3PN curve is thus entirely determined by the numerical factor A . The higher this factor is, the higher the frequency of departure. For Dey et. al. (1998) EOS, the power n is very high and the reference frequency of 1000 Hz used for the polynomial fit (7) is not well adapted to the frequency of gravitational waves obtained using this EOS, explaining the very small factor A .

From Fig. 5, we can define the frequencies f_{npm} as those frequencies at which the deviation from point-mass behavior becomes important. It can be defined more precisely by the frequency for which

$$\frac{E_{\text{bind}} - E_{\text{bind}}^{3\text{PN}}}{E_{\text{bind}}^{3\text{PN}}} = 0.001. \quad (10)$$

The values of these frequencies for the four strange star models are given in Table III.

One can draw an important conclusion from the presented results and their comparison with relativistic approximations for point masses in a binary system. We can expect that taking into account the next orders in a post-Newtonian approximation doesn't change the energy by an amount larger than the difference between 2PN and 3PN models. As a consequence the large deviation of our numerical results from the 3PN approximation is caused by the effects of a finite size of the star, e.g. tidal forces. The very high power n indicates that high order tidal effects are very important, and dominates the

EOS	M/R	$A [M_\odot]$	n	$A_{n=6.5} [M_\odot]$
SQSB40	0.1648	0.001174	6.28	0.001158
SQSB60	0.1867	0.0002888	6.59	0.0002961
SQSB56	0.1925	0.0001865	6.8	0.0002068
DSQS	0.2717	1.353e-9	17.38	–

TABLE II: Parameters A , n and $A_{n=6.5}$ (A for $n = 6.5$) of polynomial fits (7) for equal-mass of $1.35 M_\odot$ irrotational strange quark star binaries.

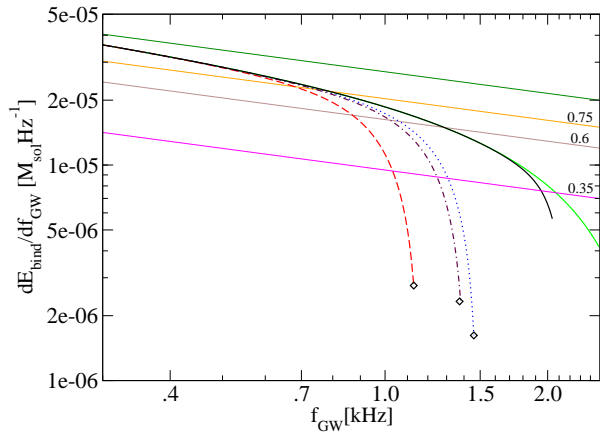


FIG. 6: Energy spectrum of gravitational waves emitted by strange stars binaries versus frequency of gravitational waves along the four equal-mass of $1.35 M_\odot$ irrotational quasiequilibrium sequences. The straight lines correspond to the Newtonian dependence of energy multiplied by 1, 0.75, 0.6 and 0.35.

relation $E_{\text{bind}}(f_{\text{GW}})$. Indeed, the lowest order tidal term is known to be $n = 4$ [62] and the values obtained here are well above this.

C. Energy spectrum of gravitational waves

We compute the energy spectrum of gravitational waves obtained as the first derivatives of the fitted functions (7). The quantity $dE_{\text{bind}}/df_{\text{GW}}$ is important for the data analysis of GW, because it determines the evolution of the wave's phase. The difference in the phase, for two $1.35 M_\odot$ strange stars described by the MIT bag model, between our numerical results and 3PN, caused by hydrodynamical effects, is $\sim 40\%$, for the last two orbits of inspiral. The phase error in the 3PN values of the wave's phase may be larger for the final orbits if one goes beyond spacial conformal flatness approximation [66].

The relation between $dE_{\text{bind}}/df_{\text{GW}}$ and the gravitational waves frequency f_{GW} is presented in Fig. 6. In this figure, we draw straight lines corresponding to the

EOS	M/R	f_{npm}	f_{25}	f_{40}	f_{65}	$f_{\text{ISCO/end}}$
SQSB40	0.1648	542	679	871	1033	1134
SQSB60	0.1867	705	744	1022	1245	1390
SQSB56	0.1925	767	756	1063	1308	1467
DSQS	0.2717	1825	786	1286	1945	2050(*)

TABLE III: Gravitational wave frequencies (in Hz) at the last orbits of inspiraling equal-mass of $1.35 M_\odot$ strange quark star binaries: f_{npm} denotes the frequency of GW at which the relative difference between binding energy calculated in quasiequilibrium and 3PN approximation is higher than 0.1%, f_{25} , f_{40} and f_{65} are the so-called break-frequencies at which the GW energy spectrum has dropped, respectively, by 25%, 40%, 65% and $f_{\text{ISCO/end}}$ is the GW frequency at ISCO for SQSB40, SQSB56, SQSB60 model and (*) at the last calculated configuration for DSQS model.

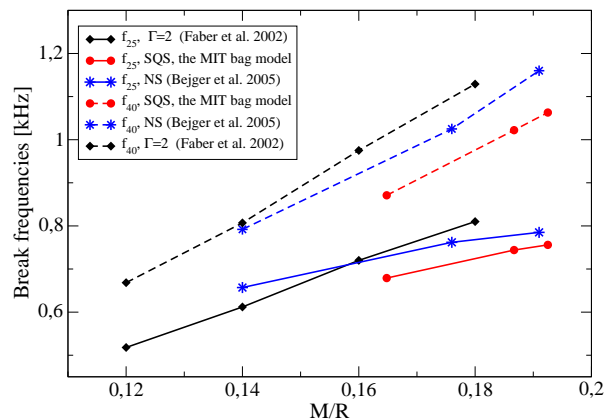


FIG. 7: The break frequencies versus compaction parameter for equal-mass (of $1.35 M_\odot$) strange stars and neutron stars described by realistic EOS [9] and polytropic EOS [5]

Newtonian case $\sim f_{\text{GW}}^{2/3}$ to find the break frequencies f_{25} , f_{40} and f_{65} at which the energy spectrum has dropped respectively by 25 %, 40 % and 65 %. The values of the break frequencies for the four EOS used to described strange stars are given in Table III. These values are important from the point of view of future detections: they show the difference between the amplitude of the real signal and the Newtonian template which allows to calculate the real wave form amplitude from the detector noise.

At the level of 25%, SQSB40 EOS is the only curve which deviate from the 3PN curve so we can already distinguish SQSB40 EOS and the other EOS. But this is only at f_{40} that we can discriminate between the four EOS, but the curve for DSQS is still very close to the 3PN curve because of very high compaction parameter for this model. To see the significant deviation of DSQS

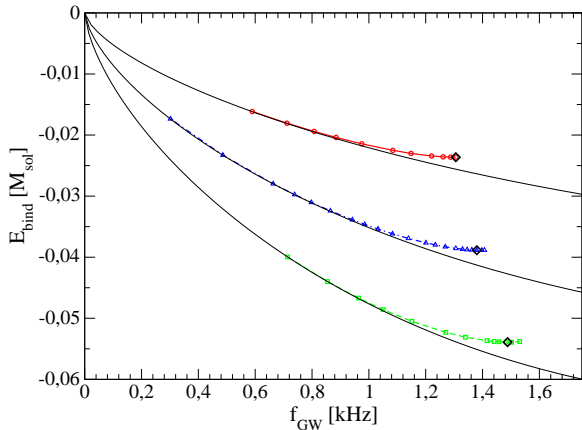


FIG. 8: Orbital binding energy E_{bind} as a function of GW frequency f_{GW} along three different total mass evolutionary sequences of irrotational binaries described by SQSB60. The total mass in infinite separation of binaries containing two identical strange stars is 2, 2.7 and $3.3 M_{\odot}$ from the top to the bottom respectively.

model from post-Newtonian results, we need to look at frequency f_{65} where the energy spectrum has dropped by 65 %.

In Fig. 7 we present the break frequencies f_{25} , f_{40} for neutron stars and strange stars described by the MIT bag model versus the compaction parameter. We find that the break frequencies are more sensitive quantities to EOS than GW frequencies at ISCO. For equal-mass binaries (of $1.35M_{\odot}$) of neutron stars described by realistic EOS the function $f_{\text{GW,ISCO}}(M/R)$ can be quite well reproduced studying neutron stars described by polytropic EOS with $\Gamma = 2$ (see Fig. 4). This isn't the case for the dependence of break frequencies versus the compaction parameter. The relation of frequencies f_{25} , f_{40} versus M/R is different for different EOS, and for given M/R always higher for neutron stars than for strange quark stars.

VI. THE IMPACT OF THE TOTAL MASS AND EOS ON THE LAST ORBITS OF INSPIRAL

Up to now, we studied the impact of the equation of state on the frequency of gravitational waves at ISCO and on break frequencies for equal-mass binaries with $M_{\infty} = 2.7M_{\odot}$. In this section, we consider equal-mass strange star binary systems with different total masses.

In Fig. 8 we show the orbital binding energy versus frequency of gravitational waves along evolutionary sequences of binary strange stars described by SQSB60

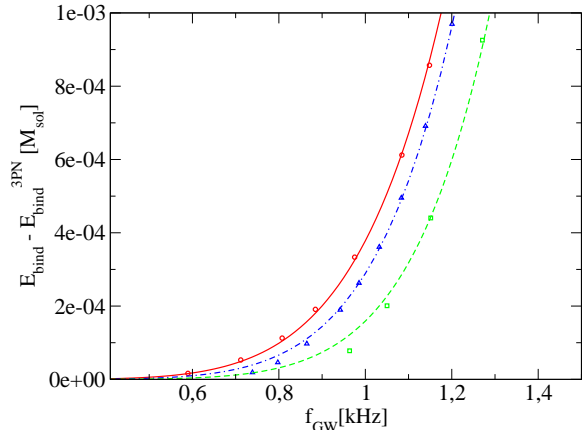


FIG. 9: $E_{\text{bind}} - E_{\text{bind}}^{3\text{PN}}$ for three irrotational strange star binaries described by SQSB60 model. The symbols correspond to the numerical results and the lines to polynomial fits to them. The total mass of binaries containing two identical strange stars is 2, 2.7 and $3.3 M_{\odot}$ from left to right respectively.

EOS with $M_{\infty} = 2 M_{\odot}$, $2.7M_{\odot}$ and $3.3M_{\odot}$.

We find a minimum of binding energy for each sequence, which corresponds to the dynamical instability. The frequency of gravitational waves at the ISCO increases with increasing total mass of equal-mass irrotational strange star binaries. We find the same behavior for other models of strange stars.

In Fig. 9 we show the difference $E_{\text{bind}} - E_{\text{bind}}^{3\text{PN}}$ between the binding energy of three equal-mass irrotational strange star binaries described by SQSB60 model and the binding energy of binary point masses in the 3PN approximation. The parameters of the polynomial fits Eq. (7) and f_{npm} frequencies for these three evolutionary sequences are given in Table IV. We find high values of the power n independently on the total mass of a binary strange star system, which indicates that tidal effects dominate the last orbits of inspiral.

$M[M_{\odot}]$	$A [M_{\odot}]$	n	f_{npm}
1	0.0003781	6.02	593
1.35	0.0002888	6.59	705
1.65	0.0001590	7.27	838

TABLE IV: Parameters A and n of polynomial fits (7) for different masses evolutionary sequences of strange stars described by SQSB60 model.

In the upper (lower) panel of Fig. 10 we show the frequency of GW at the ISCO versus gravitational mass (the compaction parameter) for three MIT bag models

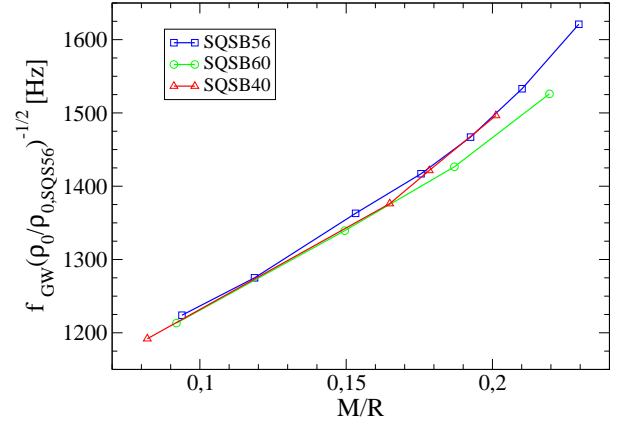
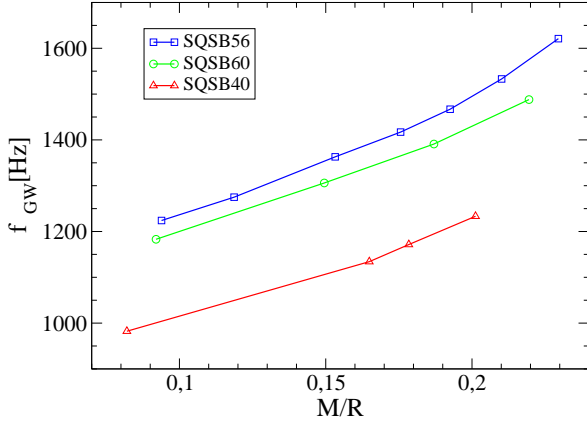
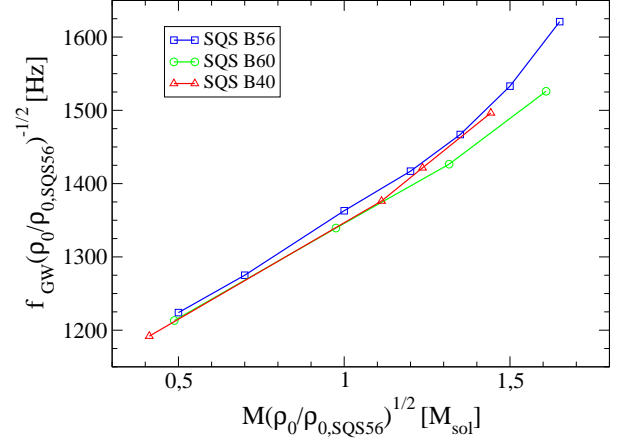
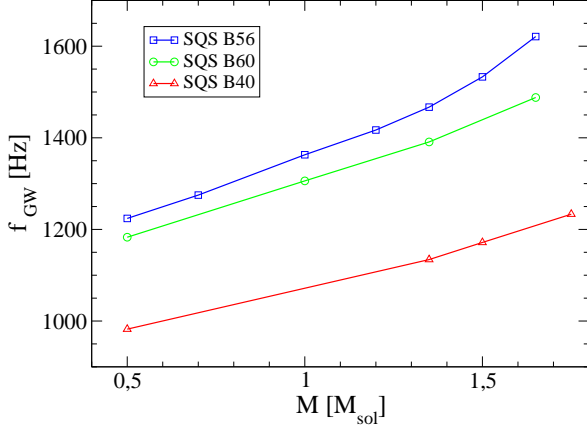


FIG. 10: The upper (lower) panel corresponds to the dependence of gravitational wave frequency at the ISCO on gravitational mass (compactness parameter) of a star in isolation for equal-mass binaries described by different strange quark matter EOS

SQSB56, SQSB60 and SQSB40. Different symbols (triangles, circles and squares) correspond to the ISCO defined by the orbital instability. We find that for all MIT bag models considered in the paper the frequency of GW at the ISCO increases with the stellar mass and the compactness parameter M/R (the relation gravitational mass vs compactness parameter is almost linear for the range of masses considered here).

It was already mention that stars built predominantly of strange quark matter described by the MIT bag model or the Dey et al. (1998) model can be very well approximated by the linear function $P = a(\rho - \rho_0)$. For a fixed value of a , all stellar parameters are subject to scaling relations with appropriate powers of ρ_0 , e.g. the gravitational mass and the stellar radius scale in the same way: $M, R \propto \rho_0^{-1/2}$ while the rotational frequency $f_{\text{rot}} \propto \rho_0^{1/2}$

FIG. 11: Upper panel (lower panel) represents the rescaled gravitational wave frequency at the ISCO as a function of the rescaled gravitational mass (compactness parameter) of a star in isolation.

(e.g. [63, 64]). In Fig. 11 the dependence of the frequency of GW at the ISCO versus mass and compactness parameter was scaled out with appropriate powers of $\rho_{0,\text{SQSB56}}$, where $\rho_{0,\text{SQSB56}} = 4.4997 [10^{14} \text{g/cm}^3]$ corresponds to the surface density for the standard MIT bag model SQSB56. We see that the functions $f_{\text{GW}}(M)$ and $f_{\text{GW}}(M/R)$ weakly depend on the a parameter of the equation of state given by Eq. (1).

In Fig. 12 and 13 we present the dimensionless quantities, the gravitational waves frequency at the ISCO multiplied by the gravitational mass of a star in isolation $M\Omega$ as a function of M/R for equal-mass strange star binaries described by the MIT bag model and neutron star binaries respectively. The frequency at the ISCO depends systematically and strongly on the compactness

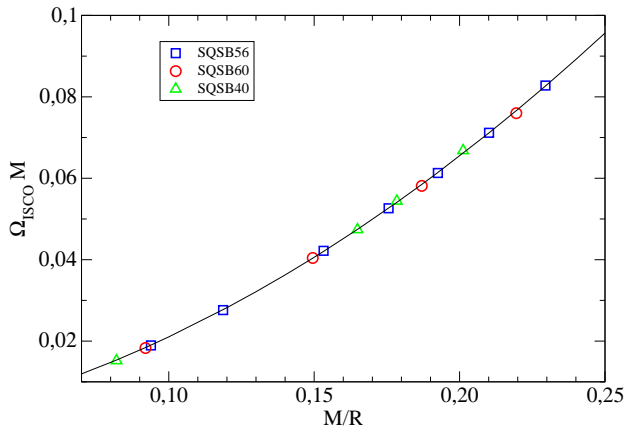


FIG. 12: The GW frequency at the ISCO multiplied by the gravitational mass of a strange star at isolation versus compaction parameter for equal-mass strange star binaries. The solid line correspond to the fitting formulae, while different symbols correspond to numerical results for different strange star models.

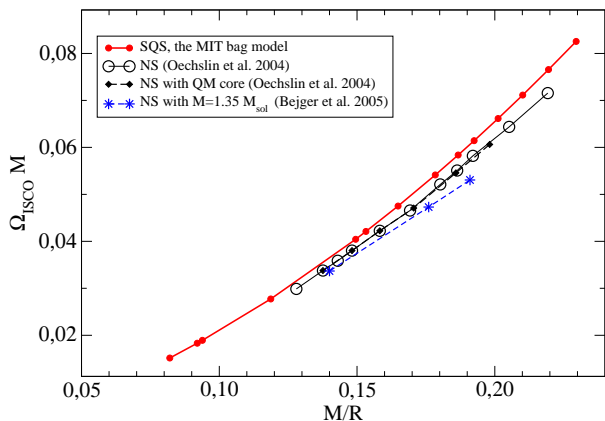


FIG. 13: The GW frequency at the ISCO multiplied by the gravitational mass versus compaction parameter for equal-mass neutron star and strange star binaries. Lines correspond to the fitting formulas, while different symbols correspond to numerical results for different strange star and neutron star models.

parameter for all models. This strong dependence for binary neutron stars and strange stars indicates that the effect of the hydrodynamic instability dominates over the general relativistic effects (see [20] for a discussion on the origin of ISCO) for compaction parameters considered in the paper. On the other hand, in the limit $M/R \rightarrow 0.5$, the general relativistic effects should be more important than the hydrodynamic effects.

We find that the dependence of the frequency of gravi-

tational waves at the ISCO on the compaction parameter for the equal-mass binaries can be described by the same simple analytical formulae (given by the power series of the compaction parameter)

$$\Omega M = A(M/R)^{1.5} + B(M/R)^{2.5}$$

(see e.g. [20, 65]), where $A = 0.6$ and $B = 0.665$, for broad ranges of masses independently on the strange star model. The results obtained for one strange quark model can then be used to predict the results for other models. Having this in mind we can estimate that the gravitational wave frequency at the ISCO $f_{\text{GW,ISCO}}$ for DSQS with $M_{\infty} = 2.7$ could be very high ~ 2.6 kHz.

Comparison of our numerical results for three different models of strange stars, represented by the solid line with filled circles, and irrotational neutron star binaries are given in Fig 13. The solid line with open circles and the dashed line with filled squares correspond to equal-mass neutron stars of Oechslin et al. 2004 [10] described by a pure nuclear matter EOS, based on a relativistic mean field model and a ‘hybrid’ EOS with a phase transition to quark matter at high density respectively. These two EOSs are matched with a polytropic one with high adiabatic index $\gamma = 2.86$ at 2×10^{14} g cm $^{-3}$. This last assumption of Oechslin et al. is artificial, because the EOS of the neutron star crust is very different from a polytrope, and its local adiabatic index is much smaller (see [9] for details). The dashed line with stars denotes results obtained by Bejger et al. 2005, for binary neutron stars of equal masses with $M_{\infty} = 2.7 M_{\odot}$ based on realistic equations of state for the whole neutron star interior (see section V. A of this paper). They performed calculations for three realistic nuclear EOSs of various softness at stellar core and the crust described by means of a realistic EOS obtained in the many-body calculations (see [9] for details). In this case ISCO is defined by the point where mass transfer sets in. In contrast for irrotational strange star binaries and neutron star binaries of Oechslin et al. the ISCO is given by the dynamical instability due to very high adiabatic index in the stellar crust (see [8]). The difference in the relation $\Omega M(M/R)$ between two models of Oechslin et al., caused by difference of EOS in the stellar core, are negligible comparing to difference between their results and our numerical calculations or results obtained by Bejger et al. The last orbits of inspiral of binary neutron stars and strange stars are dominated by tidal effects. We conclude that the difference between different models of compact stars, presented on Fig. 13 come from different description of the nuclear crust.

VII. SUMMARY

In the present paper we have computed the final phase of inspiral of equal-mass irrotational binary stars built predominantly of strange quark matter. We have studied the precoalescing stage within a quasiequilibrium approximation and a conformally flat spatial 3-metric using

a multidomain spectral method. We have presented a set of evolutionary sequences of equal-mass strange star binaries based on two types of equation of state at zero temperature, the MIT bag model and the Dey et al. (1998) model, of strange quark matter. For each sequence we have computed the gravitational waves energy spectrum. We have compared our results with those obtained for neutron star binaries and the third order Post-Newtonian point-mass binaries. We have studied the impact of the equation of state and the total energy-mass on the last orbits of binary strange quark stars by finding the gravitational wave frequency at the ISCO, which marks the end of the inspiral phase, and the break frequencies (GW frequencies at which the energy spectrum drops by some factor below the point-mass result) for each evolutionary sequence. These frequencies could be determined from data analysis and allow us to make constraints on the equation of state of neutron stars.

We find that:

i) for equal-mass irrotational strange quark star binaries ISCO is given by the dynamical instability independently on the equation of state and the total energy-mass of the system. This contrasts with neutron stars described by nuclear equation of state for which the ISCO is given by mass-shedding limit. The gravitational wave frequency at the ISCO is always higher than 1.1 kHz for irrotational strange quark stars described by MIT bag model and 2 kHz for the Dey et al. (1998) model with the total mass-energy of a binary system greater than $2M_{\odot}$. One should note here that for non-equal mass binaries a star of smaller mass could be tidally disrupted by a companion of larger mass at large orbital separation and than the frequency of gravitational waves could be smaller than 1 kHz.

ii) the frequency of gravitational waves at the ISCO depends systematically and strongly on the compaction parameter (for $M/R < 0.24$) for all models of strange quark stars. This indicates that the ISCO is determined by the hydrodynamic instability and not by general relativistic effects. The dependence of the frequency of gravitational waves at the ISCO on the compaction parameter for the equal mass binaries can be described by the same simple analytical formulae for broad ranges of masses independently on a strange star model. The higher the compactness of a star is, the higher the frequency of GW at the ISCO is.

iii) the range of GW frequencies, [1130, 1470], at the ISCO for binary strange stars of $2.7M_{\odot}$ total mass, described by the MIT bag model intersects with the range

of frequencies, [806, 1270], for binary neutron stars. The determination of the gravitational wave frequency at the ISCO by the laser interferometers wouldn't be sufficient to distinguish without ambiguities between strange stars and neutron stars. It would be necessary to take into account the observed deviation of the gravitational energy spectrum of a quasiequilibrium sequence from point-mass behavior (the break frequencies). The fits of the deviation between numerical results from 3PN results show that the power is very high, $n > 6$, which indicates that high order tidal effects are very important.

iv) The frequency of GW at the end point of inspiraling neutron stars described by several realistic EOS can be predicted, in a good approximation, by studying binaries with assumed polytropic EOSs with $\gamma = 2$ or 2.5 with the same compaction parameter. In contrast, the frequency of GW at the ISCO is always higher for strange stars binaries than for polytropic neutron stars binaries with the same compaction parameter. The differences in the evolution of binary strange stars and neutron stars stem from the fact that strange stars are principally bound by an additional force, strong interaction between quarks.

v) the higher total mass of the system is the higher frequency of GW at ISCO. For MIT bag model the frequency of gravitational waves at the ISCO only weakly depends on the parameter a of the EOS, especially for small compaction parameter. The results obtained for one model can thus be used for other MIT bag model using the scaling with ρ_0 .

In future work we plan to study binary neutron stars (strange quark stars) with different mass ratio, e.g. 0.7, following the results of [24] for the observability weighted distribution of double neutron star binaries as well as binary systems consisting of one strange star and one neutron star.

Acknowledgments

We are grateful to Koji Uryu, Thomas Baumgarte and Keisuke Taniguchi for helpful discussions and valuable comments. This work was supported, in part, by the KBN grant 1P03D00530, "Ayudas para movilidad de Profesores de Universidad e Investigadores españoles y extranjeros" from the Spanish MEC, and by the Associated European Laboratory Astro-PF (Astrophysics Poland-France).

[1] Burgay, M., et al. *Nature (London)*, **426**, 531 (2003).
 [2] V. Kalogera, C. Kim, D. R. Lorimer et al. *Astrophys. J.* **601**, 179 (2004).
 [3] K. Belczynski, V. Kalogera, and T. Bulik *Astrophys. J.* **572**, 407 (2002).
 [4] D. Lai and A. G. Wiseman, *Phys. Rev. D* **54**, 6 (1996).

[5] J. A. Faber, P. Grandclément, F. A. Rasio, and K. Taniguchi, *Phys. Rev. Let.* **89**, 231102 (2002).
 [6] K. Taniguchi and E.ourgoulhon, *Phys. Rev. D* **68**, 124025 (2003).
 [7] D. Gondek-Rosińska, Bejger, M., Bulik, T.,ourgoulhon, E., Haensel P., Limousin, F., K. Taniguchi, Zdunik, J. L.,

- Advances in Space Research, **39**, 271 (2007).
- [8] F. Limousin, D. Gondek-Rosińska, and E.ourgoulhon, Phys. Rev. D **71**, 064012 (2005).
- [9] M. Bejger, D. Gondek-Rosińska, E.ourgoulhon, P. Haensel, K. Taniguchi, and J. L. Zdunik, Astron. Astrophys. **431**, 297 (2005).
- [10] R. Oechslin, K. Uryu, G. Poghosyan, and F.K. Thielemann, Mon. Not. R. Astron. Soc. **349**, 1469 (2004).
- [11] M. Shibata, K. Taniguchi, and K. Uryu, Phys. Rev. D **71**, 084021 (2005).
- [12] C. Cutler and E.E Flanagan, Phys. Rev. D **49**, 2658 (1994).
- [13] T. W. Baumgarte and S. L. Shapiro, Phys. Rep. **376**, 41 (2003).
- [14] L. Bildsten and C. Cutler, Astrophys. J. **400**, 175 (1992).
- [15] C. S. Kochanek, Astrophys. J. **398**, 234 (1992).
- [16] S. Bonazzola, E.ourgoulhon, and J.-A. Marck, Phys. Rev. Lett. **82**, 892 (1999).
- [17] J.A. Faber, P. Grandclément, and F.A. Rasio, Phys. Rev. D **69**, 124036 (2004).
- [18] P. Marronetti, G. J. Mathews, J. R. Wilson, Phys. Rev. D **60**, 087301 (1999).
- [19] K. Uryu and Y. Eriguchi, Phys. Rev. D **61**, 124023 (2000).
- [20] K. Uryu, M. Shibata, and Y. Eriguchi, Phys. Rev. D **62**, 104015 (2000).
- [21] K. Taniguchi and E.ourgoulhon, Phys. Rev. D **65**, 044027 (2002).
- [22] P. Marronetti, M. D. Duez, S. L. Shapiro, T. W. Baumgarte, Phys. Rev. Lett. **92**, 141101 (2004).
- [23] E.ourgoulhon, P. Grandclément, K. Taniguchi, J.-A. Marck, and S. Bonazzola, Phys. Rev. D **63**, 064029 (2001).
- [24] T. Bulik, D. Gondek-Rosińska, K. Belczynski, Mon. Not. R. Astron. Soc. **352**, 1372 (2004).
- [25] Gondek-Rosińska D., Bulik, T., Belczyński, K., Proceedings of the "Stellar end products" workshop, ed. M.A. Pérez-Torres., MmSAI, **v.76**, p.632 (2005)
- [26] Dey, M., Bombaci, I., Dey, J., Ray, S., Samanta, B. C. Phys. Lett. B, **438**, 123 (1998).
- [27] F. Weber, Prog. Part. Nucl. Phys. **54**, 193 (2005).
- [28] J. Madsen, Lect. Notes Phys. **516**, 162 (1999).
- [29] D. Gondek-Rosińska, E.ourgoulhon, P. Haensel, Astron. Astrophys. **412**, 777 (2003).
- [30] P. Haensel, J.L. Zdunik, and R. Schaeffer, Astron. Astrophys. **160**, 121 (1986).
- [31] C. Alcock, E. Farhi, and A. Olinto, Astrophys. J. **310**, 261 (1986).
- [32] E. Fahri, and R. L. Jaffe, Phys. Rev. D **30**, 2379 (1984).
- [33] D. Gondek-Rosińska, T. Bulik, L. Zdunik, E.ourgoulhon, S. Ray, J. Dey, and M. Dey, Astron. Astrophys. **363**, 1005 (2000).
- [34] J. L. Zdunik, Astron. Astrophys. **359**, 311 (2000).
- [35] S. Bonazzola, E.ourgoulhon, and J.-A. Marck, Phys. Rev. D **56**, 7740 (1997).
- [36] J. L. Friedman, K. Uryu, and M. Shibata, Phys. Rev. D **65**, 064035 (2002).
- [37] J. A. Isenberg : *Waveless approximation theories of gravity*, preprint University of Maryland, unpublished (1978).
- [38] J. Isenberg and J. Nester, in *General Relativity and Gravitation*, edited by A. Held (Plenum, New York, 1980), Vol. 1.
- [39] J.R. Wilson and G.J. Mathews, in *Frontiers in numerical relativity*, edited by C.R. Evans, L.S. Finn and D.W. Hobill (Cambridge University Press, Cambridge, England, 1989).
- [40] J. W. York, in *Sources of Gravitational Radiation*, edited by L. Smarr (Cambridge University Press, Cambridge, England, 1979).
- [41] G. B. Cook, Living Rev. Rel. **3**, 5 (2000).
- [42] H.P. Pfeiffer and J.W. York, Phys. Rev. D **67**, 044022 (2003).
- [43] <http://www.lorene.obspm.fr/>
- [44] K. Taniguchi, E.ourgoulhon, and S. Bonazzola, Phys. Rev. D **64**, 064012 (2001).
- [45] K. Taniguchi and E.ourgoulhon, Phys. Rev. D **66**, 104019 (2002).
- [46] S. Bonazzola, E.ourgoulhon, and J.-A. Marck, Phys. Rev. D **58**, 104020 (1998).
- [47] L. Blanchet, Living Rev. Relativity **5**, 3 (2002).
- [48] L. Blanchet, Living Rev. Relativity, **9**, 4 (2006).
- [49] T.W. Baumgarte, G.B. Cook, M.A. Scheel, S.L. Shapiro, and S.A. Teukolsky, Phys. Rev. Lett. **79**, 1182 (1997).
- [50] M. Shibata and K. Uryu, Phys. Rev. D **61**, 064001 (2000).
- [51] M. Shibata and K. Uryu, Phys. Rev. D **64**, 104017 (2001).
- [52] M. Shibata, K. Taniguchi, and K. Uryu, Phys. Rev. D **68**, 084020 (2003).
- [53] K. Oohara and T. Nakamura, Prog. Theor. Phys. Suppl. **136**, 270 (1999).
- [54] S. A. Hughes, Phys. Rev. D **66**, 102001 (2002)
- [55] T. Damour, E.ourgoulhon and P. Grandclément, Phys. Rev. D **66**, 024007 (2002).
- [56] T. Damour, P. Jaranowski and G. Schfer, Phys. Rev. D **62**, 044024 (2000).
- [57] L. Blanchet, Phys. Rev. D **65**, 124009 (2002).
- [58] Glendenning, N. K., ApJ, **293**, 470 (1985).
- [59] Akmal, A., Pandharipande, V. R., & Ravenhall, D. G., Phys. Rev. C, **58**, 1804 (1998).
- [60] Prakash, M., Bombaci, I., Prakash, M., Ellis, P.J., Lattimer, J.M., & Knorren, R., Phys. Rep. **280**, 1 (1997).
- [61] Bombaci I., in Perspectives on Theoretical Nuclear Physics, ed. I. Bombaci, A. Bonaccorso, A. Fabrocini et al., 223 (1995).
- [62] D. Lai, F. Rasio and S.L. Shapiro, Astrophys. J. **420**, 811 (1994).
- [63] J.L. Zdunik, Astron. Astrophys. **359**, 311 (2000).
- [64] E. Witten, Phys. Rev. D **30**, 272 (1984).
- [65] T. W. Baumgarte, AIP conference proceedings, **575**, 176 (2001).
- [66] K. Uryu, F. Limousin, J. Friedman, E.ourgoulhon, M. Shibata, Phys. Rev. Lett., **97**, 171101 (2006).